



## Highlighting the role of 3C–SiC in the performance optimization of (Al,Ga)N-based High-Electron mobility transistors

Micka Bah<sup>a</sup>, Daniel Alquier<sup>a,\*</sup>, Marie Lesecq<sup>c</sup>, Nicolas Defrance<sup>c</sup>, Damien Valente<sup>a</sup>, Thi Huong Ngo<sup>b</sup>, Eric Frayssinet<sup>b</sup>, Marc Portail<sup>b</sup>, Jean-Claude De Jaeger<sup>c</sup>, Yvon Cordier<sup>b</sup>

<sup>a</sup> GREMAN, CNRS, Université de Tours, INSA Centre Val de Loire, 37071, Tours, France

<sup>b</sup> Université Côte d'Azur, CNRS, CRHEA, rue B. Grégory, 06560, Valbonne, France

<sup>c</sup> Univ. Lille, CNRS, Centrale Lille, Univ. Polytechnique Hauts-de-France, UMR 8520, IEMN-Institut d'Electronique de Microélectronique et de Nanotechnologie, F-59000, Lille, France

### ARTICLE INFO

**Keywords:**

AlN interface  
3C-SiC  
Pseudo-substrate  
SCM  
SSRM  
GaN HEMTs

### ABSTRACT

AlN nucleation layer is the key issue for the performance of GaN high frequency telecommunication and power switching systems fabricated after heteroepitaxy on Silicon or Silicon Carbide. In this work, we demonstrate and explain both the low level and the origin of propagation losses in GaN/3C-SiC/Si High Electron Mobility Transistors (HEMTs) at microwaves frequencies, in view of providing efficient circuits. First, it is shown that the use of 3C-SiC as an intermediate layer between the Si substrate and the GaN epitaxial layer drastically decreases RF propagation losses. Using Secondary Ion Mass Spectroscopy (SIMS) measurements, we demonstrate that dopant in-diffusion (both Al and Ga) into the 3C-SiC pseudo-substrate remains confined beneath the interface. Furthermore, by combining scanning capacitance microscopy (SCM) and scanning spreading resistance microscopy (SSRM), the 2D profile shows the presence of a slightly conductive zone beneath the AlN/3C-SiC interface that is highly limited (less than 50 nm) whatever the growth conditions of the (Al, Ga)N layers on 3C-SiC explaining the low propagation losses obtained for such devices. This behavior differs from the one previously observed for GaN growth on Si substrate. This work demonstrates the importance and efficiency of the 3C-SiC intermediate layer when used as a pseudo-substrate increasing not only the crystalline quality of the subsequent (Al, Ga)N layers but also permits to achieve high potential GaN power devices as it is crucial.

### 1. Introduction

GaN-based High Electron Mobility Transistors (HEMTs) are of great interest for the next generation of high frequency telecommunication and power switching applications owing to their large band gap, high breakdown field, high electron mobility, good thermal conductivity and high output power density. Furthermore, the epitaxial growth of GaN HEMTs on Silicon substrate offers the possibility to fabricate devices at relatively low cost compared to their counterparts on SiC substrate. However, the direct epitaxial growth of GaN-on-Si is difficult due to (i) high lattice mismatch and large thermo-elastic tensile strain which can induce GaN cracking, (ii) formation of undesirable  $\text{Si}_3\text{N}_4$  phase at the GaN/Si interface or (iii) Si substrate etching by Gallium that can seriously degrade materials quality. The intercalation of AlN nucleation layers between Si and GaN/Al(Ga)N based buffer layers [1] is now the foundation stone for the epitaxial growth of high quality GaN on Silicon.

Nevertheless, the electrical activity at the AlN/Si interfacial junction is still a major concern for high frequency devices performances. In high frequency operation transistors and circuits for applications such as 5G [2], it is necessary to achieve high electrical resistivity in the epilayer/substrate ensemble, especially to reach low RF losses. It is to note that not only the use of high-resistivity substrates is necessary [3], but also the achievement of both sufficient crystal quality and electrical resistivity at the AlN/Si interface is required. Among the possible origins of parasitic conductivity and propagation losses, the diffusion of dopant species into the Si substrate [4–6], the formation of an inversion layer at the AlN/Si interface [7–10] as well as the degraded crystal quality [8, 11] have been reported. In a previous study, we have shown that the nucleation of AlN on Silicon in a close coupled showerhead Metal-organic Vapor Phase Epitaxy (MOVPE) reactor was subject to Gallium memory effect which could severely limit RF performance [12]. Similarly, this effect complicates the growth of Gallium free InAlN barriers

\* Corresponding author.

E-mail address: [daniel.alquier@univ-tours.fr](mailto:daniel.alquier@univ-tours.fr) (D. Alquier).

on GaN [13]. Bulk silicon carbide (SiC) is known to be well-suited substrate for the epitaxy of GaN based HEMT structures for such RF devices, but its high cost could hence be an obstacle to a wide development of several applications. The use of cubic silicon carbide (3C-SiC) templates on Si, which may be produced at lower cost, could be highly beneficial. This alternative solution consisting in the growth of a 3C-SiC layer on Si prior to the AlN nucleation and subsequent GaN HEMT epitaxial growth (Fig. 1) has been investigated, showing clear advantages in terms of crystal quality, residual strain and RF propagation losses, that were reduced from 0.8–2 dB/mm to 0.4 dB/mm at 40 GHz [14]. The aim of the present paper is to investigate the properties of the different interfaces between grown materials to explain such a difference. To do so, the combination of several techniques is necessary to have better knowledge of the interface composition and their electrical behavior. In the present study, Secondary Ion Mass Spectroscopy (SIMS) is used to quantify the amount of impurities in the different layers and into the substrate. In addition, cross-sectional electrical analyses using Atomic Force Microscope (AFM) modes such as scanning capacitance microscopy (SCM) and Scanning Spreading Resistance Microscopy (SSRM) are performed to investigate the electrical activity at the interfaces. The combination of all these analyses correlates well with electrical results previously obtained and explains the noticeable advantage provided by 3C-SiC/Si templates for the MOVPE growth of high-performance RF HEMTs.

## 2. Materials and methods

In the present study, 0.75–0.8 μm thick 3C-SiC templates were grown at 1300 °C by Chemical Vapor Deposition in a resistively heated hot wall reactor [15] using a conventional two-step method [16]. Propane and silane precursors are used with hydrogen as carrier gas. The silicon (111)-oriented substrates with a miscut below ± 0.5° from (111) are undoped (intrinsic) with a resistivity higher than 5 kΩ cm. These 50 mm diameter Si (111) substrates are 500 μm thick. The GaN structures were grown in an Aixtron close coupled showerhead MOVPE system [14]. Table 1 describes the studied structures. In the three first studied samples (A, B and C), the buffer consists from top to substrate of a 600 nm GaN/350 nm AlGaN/200 nm AlN stack, identical for the three samples. The main difference between them is related to the preparation condition of the reactor prior to the AlN nucleation layer deposition (temperature ramp-up under H<sub>2</sub> or NH<sub>3</sub>, with or without additional H<sub>2</sub> annealing step; an additional introduction of NH<sub>3</sub> was carried out when samples were under H<sub>2</sub> conditions). In the fourth one (sample D), only

600 nm GaN and 200 nm AlN layers were grown on the 3C-SiC/Si template which was treated by chemical-mechanical polishing prior to AlN regrowth, so that the 3C-SiC thickness was slightly reduced to about 650 nm. Furthermore, to make the chemical SIMS analysis easier, a specific sample, so-called “Ref-SIMS”, consisting of a 200 nm thick AlN nucleation layer was grown with similar conditions as for sample A on a non-polished 3C-SiC/Si template. After oxide removal around 1000 °C (1200 °C thermocouple setpoint) under hydrogen flow in the MOVPE reactor, a thin (20 nm) AlN layer was nucleated at a setpoint fixed to 1100 °C. Then, the temperature was ramped up to 1200 °C setpoint range for the remaining growth of 180 nm AlN and the rest of the structure. The resulting structures on 3C-SiC/Si(111) templates are free of cracks. As shown in Table 1, the grown films are smooth with Root Mean Square (RMS) roughness between 0.5 nm and 1.5 nm for 2 × 2 μm<sup>2</sup> area atomic force AFM scans. Furthermore, the crystal quality assessed by the full width at half maximum (FWHM) of X-ray diffraction omega scan peaks (rocking curves) around symmetric (002) and asymmetric (302) GaN reflections favorably compared with one obtained for GaN grown on bare silicon as previously described in Ref. [14]. One can notice that (002) rocking curves are sensitive to threading dislocations with Burgers vector with a screw component, of pure c-type or mixed a+c type (lattice tilt) whereas the width of asymmetric (302) reflection peak is determined by the threading dislocations with an edge Burgers vector component of pure a-type or mixed a+c type (lattice twist) which are the most numerous in thick films.

RF transmission lines are fabricated using a lift-off process with electron beam evaporation of a 100 nm Ti/400 nm Au metal stack. Scattering parameters S<sub>ij</sub> were measured from 0.25 GHz up to 67 GHz using a Vector Network Analyzer (VNA) (Agilent Technologies E8361A) on lines with different lengths to assess the propagation losses.

To assess the electrical activity of the different samples, both SCM and SSRM AFM electrical modes were employed to map their 2D electrical profiles. Samples were cleaved and prepared in the configuration of angle beveling. For the SCM measurements, the samples were immersed in a H<sub>2</sub>O<sub>2</sub> solution for 20 min in order to form a thin oxide layer and to create a metal-insulator-semiconductor structure when the sample and the probe are brought together. In contrast, the SSRM samples were imaged immediately after the cleaving and cleaning in HF – H<sub>2</sub>O solution. A highly conductive Pt/Ir coated tip (SCM-PIT-V2, purchased from Bruker) with a radius of curvature of 25 nm is used for the SCM measurements. However, a heavily doped DDESP-V2 tip (purchased from Bruker) with a highly conductive diamond coating is used for the SSRM measurements to ensure an ohmic contact at the tip/

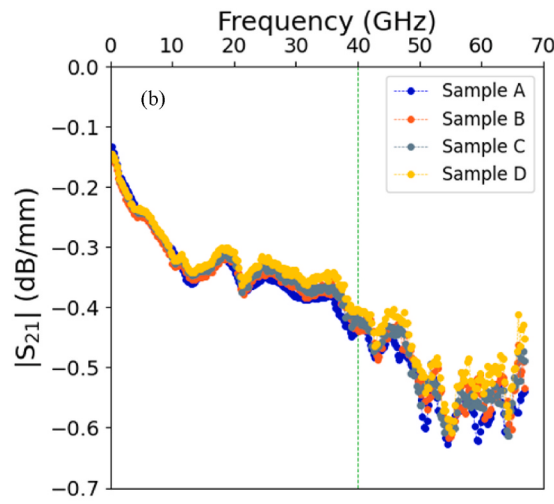
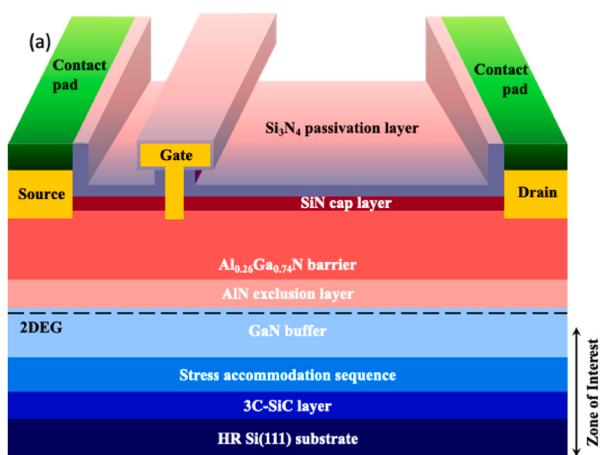


**Fig. 1.** (a) View of the zone of interest included in the full structure of an AlGaN/GaN HEMT on–3C–SiC/Si substrate (b) Propagation losses as a function of frequency for the different buffer layers grown on 3C–SiC/Si templates.

**Table 1**

Description and characteristics of the studied samples.

Sample	3C-SiC	buffer	AFM RMS (nm)	FWHM AlN 002 (°)	FWHM AlN 103 (°)	FWHM GaN 002 (°)	FWHM GaN 302 (°)
A	Not polished	600 nm GaN/350 nm AlGaN/200 nm AlN	0.8	0.55	0.55	0.37	0.54
B	Not polished	600 nm GaN/350 nm AlGaN/200 nm AlN	1.5	0.55	0.45	0.35	0.34
C	Not polished	600 nm GaN/350 nm AlGaN/200 nm AlN	–	0.53	0.58	0.37	0.71
D	3C-SiC polished	600 nm GaN/200 nm AlN	0.5	0.57	0.61	0.32	0.84
Ref-SIMS	Not polished	200 nm AlN	–	0.62	0.67	–	–

sample interface. Its nominal radius of curvature is 100 nm. During the surface scanning in contact mode, a low force of 72 nN is applied to the tip for the SCM. A force of 4  $\mu$ N is used for the SSRM to indent the native oxide which reappears on the surface of semiconductors. A 90 kHz ac bias with an amplitude of 2.5 V is applied to the sample while the tip is grounded for the SCM. A DC bias of 2.5V is used in the case of the SSRM. SCM and SSRM procedures are also described and detailed elsewhere by Bah et al. [12,17].

### 3. Results and discussions

#### 3.1. Effect of 3C-SiC buffer on the performance of the GaN-based HEMTs buffer

All the four samples (A, B, C and D) present a sheet resistance higher than the detection limit of the contactless measurement setup used for the study ( $20 \text{ k}\Omega/\text{sq}$ ). This is noticeably different from the samples previously grown on bare silicon substrates exhibiting sheet resistances below  $10 \text{ k}\Omega/\text{sq}$  [12]. RF propagation losses were extracted from  $S_{21}$  parameter measurements performed on co-planar waveguides fabricated at the surface of the grown films. As shown in Fig. 1, propagation losses increase with frequency and reach 0.4–0.44 dB/mm at 40 GHz. Considering the FWHM of GaN XRD peaks shown in Table 1, these losses obtained on structures grown on 3C-SiC/Si templates are not particularly sensitive to the GaN crystal quality and are noticeably smaller than the 0.8–2 dB/mm measured on materials grown on bare silicon substrates [12,14]. Furthermore, the losses extracted on the AlN nucleation layer of sample Ref-SIMS are slightly higher to reach 0.46 dB/mm at 40 GHz which may be due to the much lower distance of 200 nm between the metal waveguide and the silicon substrate compared to previous

samples (800–1150 nm). Altogether, these results indicate that, in the present samples, the main part of losses is not generated by the GaN or AlGaN layers growth. Khediri et al. [18] have shown that the addition of 3C-SiC in the heterostructure of GaN – based HEMTs is a useful approach to reduce the leakage current in such device compared to the conventional one grown on Si. They observed from Technology Computer-Aided Design (TCAD) simulation that the 3C-SiC layer suppresses the interface buffer/Si-substrate current path and helps to improve the breakdown voltage. In the present work, we confirm this observation by nano-electrical characterization at the interfaces of the materials.

#### 3.2. SIMS analyses

As mentioned previously, a specific sample “Ref-SIMS” was grown for such analyses. SIMS profiles have been obtained using a 14 keV Cs<sup>+</sup> ion beam for N, C and Si elements while a 3 keV O<sub>2+</sub> ion beam is used for Al, Ga and Si. In such case, Si element is taken as common reference for the analyses. The plots of Si, C and N elements were used to locate the different interfaces i.e. the aluminum nitride, the silicon carbide layers and the silicon substrate (Fig. 2b). As shown in Fig. 2a, a noticeable amount of gallium is present at the interface between AlN and 3C-SiC layers. As previously discussed in Ref. [12], this effect is related to a memory effect in the MOVPE reactor and the same effect occurs at the AlN/Si interface, as shown on SIMS results in Fig. 3a, taken on one of ref. [12] sample. The comparison with Fig. 2 shows that the concentration of gallium drops down also in the 3C-SiC layer but reaches rapidly a low doping level. To confirm Ga and Al profiles and such low concentrations, it would be of interest to completely etch the Si substrate and perform a SIMS measurement from the former SiC/Si interface to the surface [19].

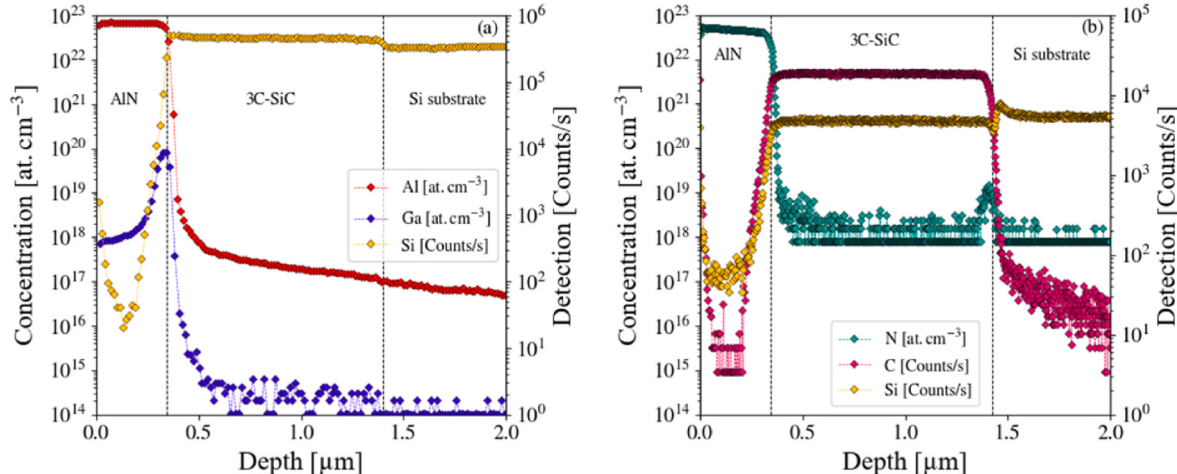
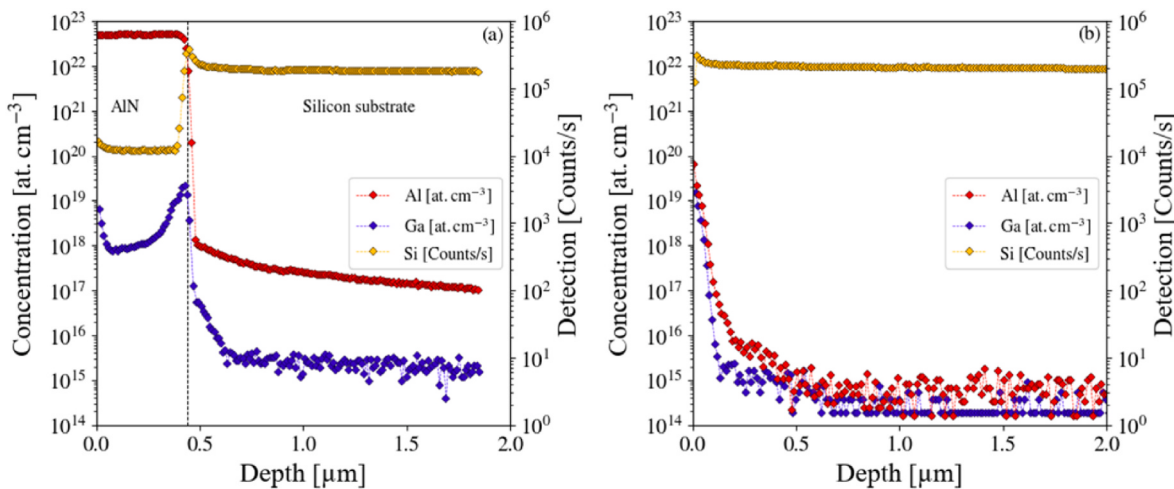


Fig. 2. SIMS profiles of (a) Al and Ga (b) N concentrations across the AlN/3C-SiC/Si layers using the sample Ref-SIMS. Si and C counts are plotted to locate the different layers and interfaces.



**Fig. 3.** SIMS profiles of Al and Ga concentrations across the AlN/Si interface (a) before and (b) after the dry etching of the AlN layer (Sample taken from Ref. [12]).

Furthermore, Fig. 3b reminds that, even after dry etching of the whole AlN layer, gallium and aluminum are detected in the silicon substrate close to the interface with AlN before the concentration levels drop but remain at a level higher to the detection limit for more than half of a micrometer.

### 3.3. Nanoelectrical activity at material interfaces

Understanding the electrical activity at the interfaces is crucial and AFM electrical modes are an ideal tool to do so. We have used here both SCM and SSRM measurements. A low roughness is necessary to minimize the tip-sample contact area as it can affect the electrical response. Fig. S1 in the supplementary information displays the topography and deflection error signal for samples A, B, C and D. The root mean square roughness is in between 1 and 4.5 nm, which is very low compared to the radius of curvature of the tips used (25 nm for the SCM Tip and 100 nm for the SSRM tip). A shallow crevice is visible at the heterostructure interfaces. To dissociate their effect from that of an inversion of the majority carrier, the bevel angle has been further reduced to better spread out the area of interest underneath the interfaces for specific sample. Besides, in our previous work [12], it was evidenced that the

diffusion of nonintentional extrinsic dopants (Ga and/or Al) induced p-type conductive channels beneath the AlN/Si interface, which increase the propagation losses in GaN-on-Si HEMTs. Reducing or inhibiting these sources of losses is necessary to improve the high-frequency device performance. An original approach is to lower the deposition temperature but this is associated to a lower crystal quality, which also affects the device performance. At present, 3C-SiC layer is intercalated between the AlN buffer and the Si substrate and its effect on the dopant diffusion is explored thanks to the electrical modes of the scanning probe microscopy. The cross section of the (Al,Ga)N-based HEMT multilayer structure is prepared by FIB as illustrated in Fig. 4A. Such heterostructure (corresponding to sample A) consists of a 3C-SiC/Si template on which AlN, AlGaN and GaN layers are successively grown. The lateral resolution of the SCM depends on the depletion region, which, in turn, is few times the Debye screening length [17,20]. For a low doping level, the Debye length is equal or higher than the diffusion depth leading to a poor spatial resolution. In this context, the different samples are prepared in the configuration of angle beveling to expand the area of interest. Such configuration is also beneficial to enhance the lateral resolution of the SSRM, which corresponds to the radius of curvature of the tip.

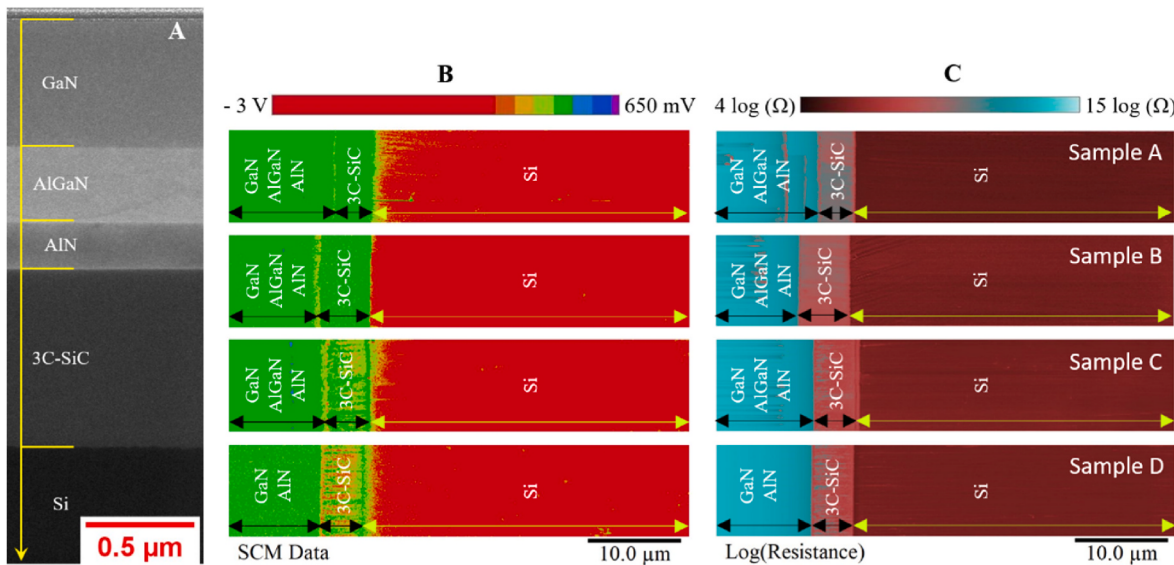


**Fig. 4.** Image A represents a SEM cross-section of the AlGaN/GaN HEMT grown on AlN/3C-SiC/Si substrate corresponding to sample B. Panels B and C show local capacitance variations (SCM) and local resistance (SSRM) across beveled surfaces of AlGaN/GaN heterostructures on AlN/3C-SiC/Si substrates for samples A–D.

**Fig. 4B** shows nanoscale capacitance variations (SCM) whereas **Fig. 4C** represents the local resistance (SSRM) across the beveled surfaces of AlGaN/GaN HEMTs grown on AlN/3C-SiC/Si substrates for samples A–D. Let us first consider the SCM data (**Fig. 4.B**). The lock-in amplifier is set-up using a SRAM normalized test sample (purchased from Bruker) so that the negative signal corresponds to the n-type doping and the positive signal to the p-type. The SRAM structures consists of NMOS and PMOS implant regions onto a silicon wafer. Such regions are associated with n-type implants into the p-epi layer and p-type implants in the n-well. The doping levels for these structures are in between  $2 \times 10^{16}$  and  $2 \times 10^{20}$  at  $\text{cm}^{-3}$ . It is worth noting that the absolute value of the SCM signal (or amplitude) is inversely proportional to the dopant concentrations. First, the GaN and AlGaN layers (green color), having probably experienced surface state modification after beveling, do not show electrical activity for all samples. Note that GaN based compounds show electrical activity when they are prepared in the cross-section configuration by cleaving. Such observations are usually found on GaN materials, as reported in Ref. [21] for example. Second, AlN (green color) that is a dielectric/piezoelectric material without modifiable charge carrier under AC field is definitely not active during SCM. Third, the 3C-SiC layer (green color) shows weak SCM signal variations, which can be correlated to a poor lateral resolution. Indeed, a highly resistive SiC with a low residual carrier level would comply with a high Debye screening length and thereby to a fully depleted SiC layer along its thickness and to an extended depletion layer in the lateral direction. Negative SCM signal obtained on samples C and D indicated that the SiC layer is of n-type while for samples A and B the signal is quantitatively non-significant. This corresponds to the electronic noise of the SCM module. Finally, the Si substrate exhibits a uniform and constant SCM signal, which can be associated with a constant depletion area underneath the tip. The negative SCM signal indicates a n-type doping. Moreover, the high SCM signal amplitude indicates that the Si substrate (orange color) is lowly doped. Next, when considering the SSRM signal (**Fig. 4C**), GaN and/or AlGaN/AlN layers show a high local resistance value while the 3C-SiC has an intermediate local resistance between those of AlN and Si. The local resistance signal is uniform over the different SiC and Si layers.

To better visualize the material interfaces, 1D SCM and SSRM profiles (**Fig. 5.A** and **B**) are extracted from the 2D images shown in **Fig. 4.B** and **C**. First, the negligible capacitance variations (SCM signal) and the high local resistance (SSRM) for the GaN and AlGaN/AlN layers inform that they are not conducting, in line with the information already

mentioned above (related to beveling). Second, the local resistance in the 3C-SiC layer in between  $10^8$  and  $10^{10}$   $\Omega$  for samples A–D while their corresponding local capacitance variations are not well defined. The difficulty of creating a thin oxide layer on the top surface of 3C-SiC (by wet oxidation in  $\text{H}_2\text{O}_2$  solution) or the formation of an extended depletion layer underneath the tip can explain the very low amplitude or absence of SCM signals. The abrupt electrical activity transition between the 3C-SiC layer and the Si substrate visible from the SCM/SSRM signals provides strong evidence that there is no quantitatively significant active dopant diffusion at their interface or parasitic conductive channel formation, which is beneficial for limiting the RF propagation losses in the corresponding HEMT devices. It is worth emphasizing that the inversion point of the SCM signal underneath the interfaces is not well resolved probably due to a large depletion region combined to a tip average effect. For these reasons, or due to the shallow depth of diffusion below the interfaces, which is less than or equivalent to the lateral resolution, it is not possible to evidence an inversion of the majority carrier. The short electrical signal vanishing at the GaN/AlGaN, AlGaN/AlN and AlN/SiC interfaces can be associated with the increase in the tip/sample contact surface and/or the interdiffusion process in solid phase between the different layers. Dissociating these two effects is difficult. To dissociate the diffusion effect beneath the interface to the topographic one, the host layer must be electrically active. Imaging the charge carrier profile in the GaN and AlGaN layers after the polishing step or the FIB preparation is not possible due to their surface state modification [21]. The 2D mapping of their electrical activity profile along the cross section is only possible after a cleaving process. However, their reduced depths offer a poor spatial resolution and do not permit accurate imaging of the interfaces. Otherwise, the increase in the contact surface at the interface is often observed between layers if their mechanical hardness is different, which induces a crevice during mechanical polishing and increases the collected current. Besides, the accurate determination of the depth over which the electrical activity vanishes is not easy due to such a change at the surface.

In order to study, in more details, the interfaces AlN/3C-SiC/Si, additional characterizations were performed. Indeed, the heteroepitaxial growth of 3C-SiC on Si is known to create defects that may propagate all along the 3C layer [15,16]. The defects can be of various types (stacking faults (SF), micro-twins and antiphase domains). As it can be easily observed in **Fig. 6.A**, the SFs defects may tend to annihilate when increasing 3C-SiC film thickness. A SF linear density up to  $10^4 \text{ cm}^{-1}$  is generally observed in 1  $\mu\text{m}$  thick layer. In previous work [22],

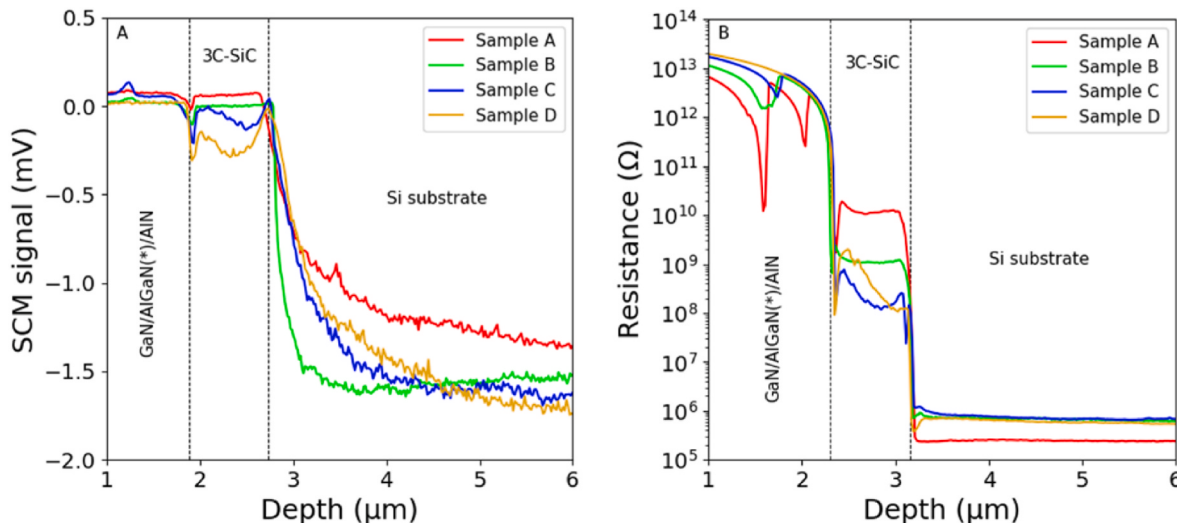


**Fig. 5.** One-dimensional electrical profiles for samples A–D obtained from mean values of  $512 \times 128$  scan lines. Panel A corresponds to local capacitance variations (SCM) while panel B represents local resistances (SSRM). The lateral dimension along the bevel direction is converted into real distance by dividing it by  $1/\sin\alpha$  ( $\alpha$  being the bevel angle).

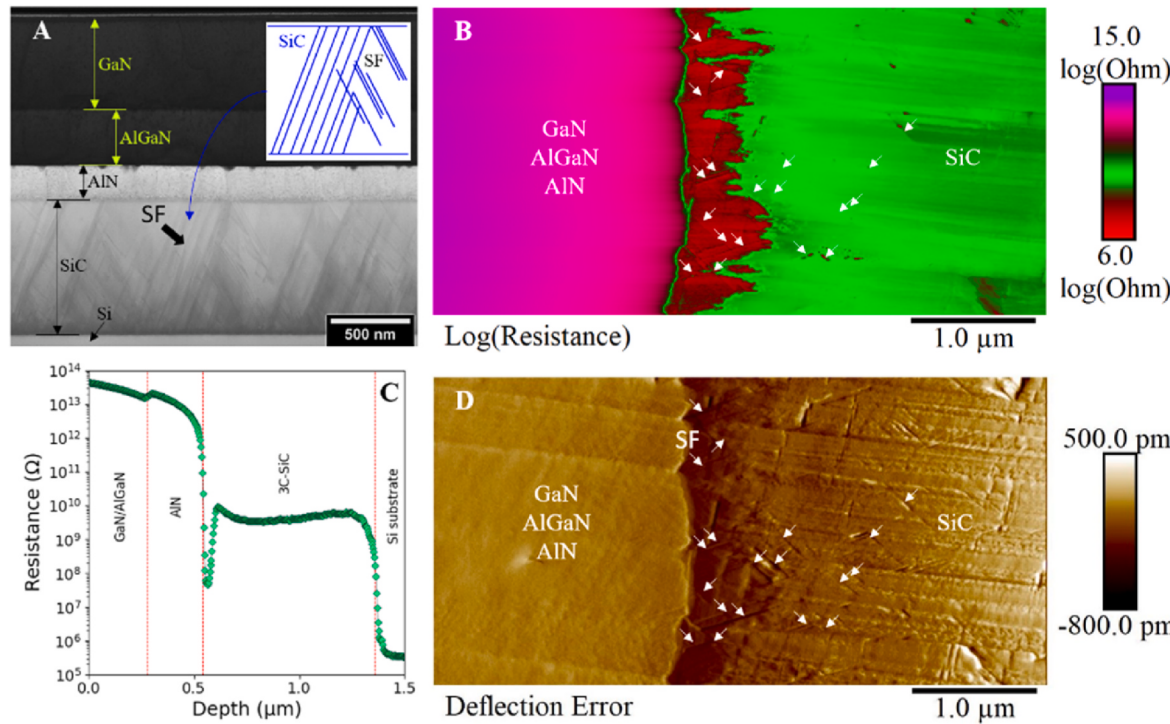


**Fig. 6.** Nanoelectrical activity at the AlN/3C-SiC interface for sample B. Image A is a STEM cross section evidencing the presence of arrays of stack faults along the 3C-SiC template. B represents the 2D SSRM profile. A thin-doped layer (burgundy color) beneath the AlN buffer associated to Al and/or Ga diffusions is visible inside the 3C-SiC template (green color). The real distance is magnified up to 12 times after angle beveling. The arrows point out the electrically active stack faults. C corresponds to the 1D SSRM profile across the AlN/3C-SiC/Si layers after distance conversion. Image D is the deflection error signal.

using AFM electrical mode, we have shown that these SFs can act as a sink for the dopants and clearly affect the electrical activity in the 3C-SiC layer, creating a full electrical path along the layer. Ga and/or Al, that are dopants for both SiC and Si may diffuse through the SFs and, hence, induce the formation of a parasitic channel, leading inevitably to propagation losses in the HEMT devices using SiC buffer. To evaluate such effect, SSRM analyses were performed and are presented in Fig. 6.B and C. Surprisingly, SFs are clearly visible in the deflection error signal shown in Fig. 6.D despite the presence of few polishing scratches. Note that the local root mean square is less than 3 nm. It can be observed that the Ga or Al in-diffusion may occur only in a few tens of nm (<50 nm) where the SSRM signal drastically decreases (Fig. 6.C). The 3C-SiC layer and the associated SFs are active only in the extremely reduced zone (burgundy color in Fig. 6.B) while the rest of the layer (green color) remains highly resistive. Furthermore, none electrical activity crossing the entire 3C-SiC layer through the SFs is observed here, as it was the case in previous work [22]. This means that if a parasitic channel exists, it is confined in less than 50 nm at the AlN/SiC interface. Such parasitic channel, which is very low compared to the ones reported in our previous work for the AlN-on-Si samples grown at different temperatures [12] will have a very low influence on the propagation RF losses. However, these losses remain a little bit too high compared to those on semi-insulating 4H-SiC (typically less than 0.2 dB/mm at 40 GHz). This could be related to losses in Si substrate that is brought during high temperature growth of 3C-SiC, that may lead to the presence of thermal donors as already shown in the literature [23]. Further investigations are required to understand this phenomenon and improve (Al,Ga)N devices on 3C-SiC/Si pseudo-substrates.

#### 4. Conclusion

In this work, the interest of the 3C-SiC as pseudo-substrate for high performance RF GaN HEMT devices is demonstrated. First, on an electrical point of view, highly efficient HEMTs were obtained with

propagation losses as low as 0.4 dB/mm at 40 GHz permitting to enhance this performance by a factor 2 to 5 compared with those on Si substrates. Both chemical (SIMS) and electrical (SCM, SSRM) profiling approaches were performed for better understanding of the HEMT electrical performances. First, SIMS analyses show that accumulation of dopant (both Al and Ga) during the growth exists, but in-diffusion of the species seems to be limited around the AlN/3C-SiC interface. Furthermore, SCM and SSRM data highlight that, for all samples, doping variations are extremely limited to a very shallow depth beneath the AlN/3C-SiC interface. Through high-resolution AFM electrical imaging, we demonstrate that this dopant in-diffusion do not exceed 50 nm beneath the interface and that the defects observed in the 3C-SiC layer do not act as a free path for Ga and/or Al dopants. Hence, the parasitic channel that may influence the electrical characterization is extremely small. The 3C-SiC layer acts, as expected, as a perfect pseudo-substrate for both crystal growth and device performance. This is a very promising result for the development of efficient (Al,Ga)N low cost devices.

#### CRediT authorship contribution statement

**Micka Bah:** Writing – review & editing, Writing – original draft, Software, Methodology, Investigation. **Daniel Alquier:** Writing – review & editing, Writing – original draft, Methodology, Funding acquisition, Conceptualization. **Marie Lesecq:** Writing – review & editing, Investigation. **Nicolas Defrance:** Writing – review & editing, Investigation. **Damien Valente:** Writing – review & editing, Investigation. **Thi Huong Ngo:** Writing – review & editing, Investigation. **Eric Frayssinet:** Writing – review & editing, Writing – original draft, Investigation. **Marc Portail:** Writing – review & editing, Investigation. **Jean-Claude De Jaeger:** Writing – review & editing, Methodology, Funding acquisition, Conceptualization. **Yvon Cordier:** Writing – review & editing, Writing – original draft, Methodology, Investigation, Funding acquisition, Conceptualization.

## Declaration of competing interest

The authors declare that they have no known competing financial interests or personal relationships that could have appeared to influence the work reported in this paper.

## Data availability

No data was used for the research described in the article.

## Acknowledgements

This work was supported by the technology facility network RENATECH, the French National Research Agency (ANR) through the projects ASTRID GoSiMP (ANR-16-ASTR-0006-01) and the “Investissement d’Avenir” program GaNeX (ANR-11-LABX-0014). Author works (MB, DA) have also been supported by GaN4AP project from the Electronic Component Systems for European Leadership Joint Undertaking (ECSEL JU), under grant agreement No.101007310. This has received financial support from GaN4AP.

## Appendix A. Supplementary data

Supplementary data to this article can be found online at <https://doi.org/10.1016/j.mssp.2023.107977>.

## References

- [1] A. Watanabe, T. Takeuchi, K. Hirosawa, H. Amano, K. Hiramatsu, I. Akasaki, The growth of single crystalline GaN on a Si substrate using AlN as an intermediate layer, *J. Cryst. Growth* 128 (1993) 391, [https://doi.org/10.1016/0022-0248\(93\)90354-Y](https://doi.org/10.1016/0022-0248(93)90354-Y).
- [2] F. Iucolano, T. Boles, GaN-on-Si HEMTs for wireless base stations, *Mater. Sci. Semicond. Process.* 98 (2019) 100, <https://doi.org/10.1016/j.mssp.2019.03.032>.
- [3] E.M. Chumbes, A.T. Schremer, J.A. Smart, Y. Wang, N.C. MacDonald, D. Hogue, J. J. Komiak, S.J. Lichwalla, R.E. Leoni, J.R. Shealy, AlGaN/GaN high electron mobility transistors on Si(111) substrates, *IEEE Trans. Electron. Dev.* 48 (2001) 420, <https://doi.org/10.1109/16.906430>.
- [4] P. Rajagopal, J.C. Roberts, J.W. Cook Jr., J.D. Brown, E.L. Piner, K.J. Linthicum, Mocvd algan/gan hfets on si: challenges and issues, *Mater. Res. Soc. Symp. Proc.* 798 (2004) 61, <https://doi.org/10.1557/PROC-798-Y7.2>.
- [5] S. Hoshi, M. Itoh, T. Marui, H. Okita, Y. Morino, I. Tamai, F. Toda, S. Seki, T. Egawa, 12.88 W/mm GaN high electron mobility transistor on silicon substrate for high voltage operation, *Appl. Phys. Express* 2 (2009), 061001, <https://doi.org/10.1143/APEX.2.061001>.
- [6] S. Chang, M. Zhao, V. Spampinato, A. Franquet, L. Chang, The influence of AlN nucleation layer on RF transmission loss of GaN buffer on high resistivity Si (111) substrate, *Semicond. Sci. Technol.* 35 (2020), 035029, <https://doi.org/10.1088/1361-6641/ab7149>.
- [7] H. Yacoub, D. Fahle, M. Finken, H. Hahn, C. Blumberg, W. Prost, H. Kalisch, M. Heuken, A. Vescan, The effect of the inversion channel at the AlN/Si interface on the vertical breakdown characteristics of GaN-based devices, *Semicond. Sci. Technol.* 29 (2014), 115012, <https://doi.org/10.1088/0268-1242/29/11/115012>.
- [8] T.T. Luong, F. Lumbantoruan, Y.-Y. Chen, Y.-T. Ho, Y.-C. Weng, Y.-C. Lin, S. Chang, E.-Y. Chang, RF loss mechanisms in GaN-based high-electron-mobility-transistor on silicon: role of an inversion channel at the AlN/Si interface, *Phys. Status Solidi* 214 (2017), 1600944, <https://doi.org/10.1002/pssa.201600944>.
- [9] H. Chandrasekar, K.N. Bhat, M. Rangarajan, S. Raghavan, N. Bhat, Thickness dependent parasitic channel formation at AlN/Si interfaces, *Sci. Rep.* 7 (2017), 15749, <https://doi.org/10.1038/s41598-017-16114-w>.
- [10] H. Chandrasekar, M.J. Uren, M.A. Casbon, H. Hirshy, A. Eblabla, K. Elgaid, J. W. Pomery, P.J. Tasker, M. Kuball, Quantifying temperature-dependent substrate loss in GaN-on-Si RF technology, *IEEE Trans. Electron. Dev.* 66 (2019) 1681, <https://doi.org/10.1109/TED.2019.2896156>.
- [11] F. Berber, D.W. Johnson, K.M. Sundqvist, E.L. Piner, G.H. Huff, H. Rusty Harris, RF dielectric loss due to MOCVD aluminum nitride on high resistivity silicon, *IEEE Trans. Microw. Theor. Tech.* 65 (2017) 1465, <https://doi.org/10.1109/TMTT.2017.2656865>.
- [12] M. Bah, D. Valente, M. Lesecq, N. Defrance, M.G. Barros, J.C. De Jaeger, E. Frayssinet, T.H. Ngo, D. Alquier, Y. Cordier, Electrical activity at the AlN/Si Interface: identifying the main origin of propagation losses in GaN-on-Si devices at microwave frequencies, *Sci. Rep.* 10 (2020), 14166, <https://doi.org/10.1038/s41598-020-71064-0>.
- [13] M. Mrad, M. Charles, Y. Mazel, E. Nolot, J. Kanyandekwe, M. Veillerot, P. Ferret, G. Feuillet, Understanding and controlling Ga contamination in InAlN barrier layers, *J. Cryst. Growth* 507 (2019) 139, <https://doi.org/10.1016/j.jcrysgro.2018.10.039>.
- [14] E. Frayssinet, L. Nguyen, M. Lesecq, N. Defrance, M. Garcia Barros, R. Comyn, T. H. Ngo, M. Zielinski, M. Portail, J.-C. De Jaeger, Y. Cordier, Metalorganic chemical vapor phase epitaxy growth of buffer layers on 3C-SiC/Si(111) templates for AlGaN/GaN high electron mobility transistors with low RF losses, *Phys. Status Solidi A* 217 (2020), 1900760, <https://doi.org/10.1002/pssa.201900760>.
- [15] T. Chassagne, A. Leycuras, C. Balleaud, P. Arcade, H. Peyre, S. Juillaguet, Investigation of 2 inch SiC layers grown in a resistively-heated LP-CVD reactor with horizontal "Hot-Walls", *Mater. Sci. Forum* 457/460 (2004) 273, <https://doi.org/10.4028/www.scientific.net/MSF.457-460.273>.
- [16] S. Nishino, J.A. Powell, H.A. Will, Production of large-area single-crystal wafers of cubic SiC for semiconductor devices, *Appl. Phys. Lett.* 42 (1983) 460, <https://doi.org/10.1063/1.193970>.
- [17] M. Bah, T.S. Tlemcani, S. Boubenia, C. Justeau, N. Vivet, J.M. Chauveau, F. Jomard, K. Nadraud, G. Poulin-Vitrant, D. Alquier, Assessing the electrical activity of individual ZnO nanowires thermally annealed in air, *Nanoscale Adv.* 4 (2022) 1125, <https://doi.org/10.1039/DINA00860A>.
- [18] A. El Hadi Khediri, B. Benbakhti, J.-C. Gerbedoen, H. Maher, A. Jaouad, N. E. Bourzgui, A. Soltani, Dual role of 3C-SiC interlayer on DC and RF isolation of GaN/Si-based devices, *Appl. Phys. Lett.* 121 (2022), 122103, <https://doi.org/10.1063/5.0102644>.
- [19] L. Wei, X. Yang, J. Shen, D. Liu, Z. Cai, C. Ma, X. He, J. Tang, S. Qi, F. Xu, X. Wang, W. Ge, B. Shen, Al, Diffusion at AlN/Si interface and its suppression through substrate nitridation, *Appl. Phys. Lett.* 116 (2020), 232105, <https://doi.org/10.1063/5.0006496>.
- [20] W.C. Johnson, P.T. Panousis, The influence of debye length on the C-V measurement of doping profiles, *IEEE Trans. Electron. Dev.* 18 (1971) 965, <https://doi.org/10.1109/T-ED.1971.17311>.
- [21] M. Lamhamdi, F. Cayrel, A.E. Bazin, E. Collard, D. Alquier, Carrier profiling in Si-implanted gallium nitride by scanning capacitance microscopy, *Nucl. Instrum. Methods Phys. Res. Sect. B Beam Interact. Mater. Atoms* 275 (2011) 37, <https://doi.org/10.1016/j.nimb.2011.12.003>.
- [22] X. Song, J.F. Michaud, F. Cayrel, M. Zielinski, M. Portail, T. Chassagne, E. Collard, D. Alquier, Evidence of electrical activity of extended defects in 3C-SiC grown on Si, *Appl. Phys. Lett.* 96 (2010), 142104, <https://doi.org/10.1063/1.3383233>.
- [23] S. Ghosh, A. Hinz, S.M. Fairclough, B.F. Spiridon, A. Eblabla, M.A. Casbon, M. J. Kappers, K. Elgaid, S. Alam, R.A. Oliver, D.J. Wallis, Origin(s) of anomalous substrate conduction in MOVPE-grown GaN HEMTs on highly resistive silicon, *ACS Appl. Electron. Mater.* 3 (2) (2021) 813–824, <https://doi.org/10.1021/acsaelm.0c00966>.